Optimal Placement of GIC Blocking Devices Considering Equipment Thermal Limits and Power System Operation Constraints

Afshin Rezaei-Zare, *Senior Member, IEEE*, and Amir H. Etemadi, *Member, IEEE*

***Abstract*—A practical mitigation of the geomagnetic disturbance (GMD) consequences in power systems is not possible without taking into account the equipment thermal limits and operational constraints. This paper presents such limitations, develops the required equations and characteristics, and proposes a general and comprehensive approach to incorporate these limits in any short-term or long-term geomagnetically induced current (GIC) mitigating solution. As an application, this study formulates the limits in the context of an optimal placement of the GIC blocking devices at the neutral point of the power transformers in the IEEE 118-bus benchmark study system. The proposed optimization problem takes into account synchronous generator real/reactive power capability, acceptable bus voltage magnitudes, transformer hot-spot heating, transmission-line thermal limits, capacitor bank harmonic loading, and synchronous generator rotor heating. This paper shows that the existing standards significantly underestimate the generator rotor heating under the GMD conditions and propose more accurate alternatives. The study results show that considering the equipment thermal limits results in a noticeably different solution when compared with the case of ignoring such limits.**

***Index Terms*—Geomagnetic disturbances (GMD), geomagnetically induced current (GIC), GIC blocking device, voltage stability, transformer saturation.**

I. Introduction

THE FLOW of geomagnetically-induced current (GIC) in power system, during a Geomagnetic Disturbance (GMD), can result in detrimental impacts on power systems. Severe consequences of GIC flow in power systems have long been known [1]. The Hydro-Quebec power system blackout and the failure of a Generator Step-Up (GSU) transformer in Salem nuclear plant, New Jersey, on March 13, 1989 are examples of such consequences [1]. To mitigate GMD adverse impacts, short-term and long-term remedies can be pursued [1], [2]. Short-term remedies mainly focus on operational preventive or corrective actions such as increasing situational awareness, increasing system margins, and reconfiguring the power system by switching in/out the transformers and transmission lines. The system topology changes can also be required due to forced outages resulting from either equipment failures or alarming during the GMD. Whether planned or forced, the outages impact the loading conditions of the other in-service equipment and the system voltage profile, and to avoid cascading outages, the equipment limits and system constraints should be taken into account in the associated contingency analysis. Although the existing commercial software packages for power system analysis typically consider the equipment loading limits, such limits are based on the normal loading conditions and therefore irrelevant to and significantly different from the equipment duty during GMD conditions. Unlike the conventional loading limits, the GMD-caused thermal stresses are mainly due to the transformer core saturation and the flow of harmonic currents in the system.

The long-term solutions primarily include the installation of GIC Blocking Devices (BDs) which eliminate the GIC flow in power system. One of the widely considered type of the BDs include those installed at neutral point of the transformers [3]. However, the installation of such a BD on a particular transformer redirects the flow of GIC to the neighboring transformers and can potentially exacerbate the power system operating conditions. Consequently, the placement of BDs should be viewed as an optimization problem that minimizes the number of installed BDs while ensuring acceptable operation conditions for the power apparatus and system.

Nevertheless, the BD placement approaches proposed in the technical literature fail to take into account the equipment GIC thermal limits. The optimal BD placement was first presented in [4], where a genetic algorithm approach was employed to minimize the number of BDs in the modified IEEE 118-bus benchmark power system while ensuring that the generator real/reactive power and the system voltages are maintained within permissible ranges. The numerical results show the effectiveness of the proposed scheme for reducing adverse GMD impacts on the system under study [4]. The BD placement is also discussed in [5] where the sensitive transformers are identified first and then a linearized objective function is used to optimally place BDs on the pre-identified transformers. However, a practical and effective GIC mitigation approach which accounts for both system power/voltage constraints and equipment thermal limits is still lacking.

Manuscript received October 20, 2016; revised March 17, 2017; accepted May 20, 2017. Date of publication June 2, 2017; date of current version January 22, 2018. Paper no. TPWRD-01245-2016. *(Corresponding author: Amir H. Etemadi.)*

A. Rezaei-Zare is with the Department of Electrical Engineering and Computer Science, York University, Toronto ON M3J 1P3, Canada (e-mail: rezaei@cse.yorku.ca).

A. H. Etemadi is with the Department of Electrical and Computer Engineering, The George Washington University, Washington, DC 20052 USA (e-mail: etemadi@gwu.edu).

Color versions of one or more of the figures in this paper are available online at http://ieeexplore.ieee.org.

Digital Object Identifier 10.1109/TPWRD.2017.2711502

Based on the IEEE 118-bus benchmark system [6], this paper presents a BD placement algorithm with an optimization objective function considering a number of crucial equipment and operating constraints. By integrating all these constraints in the optimization problem, this paper proposes a more realistic solution to minimize the GMD impacts on power systems. The numerical results indicate that by considering the equipment thermal limits, noticeably higher number of the BDs are required compared with the case of ignoring these limits. This may completely change the planning and operation strategy dealing with GMDs.

II. GMD Impacts on Power System Equipment

This section presents the impacts of GMDs on power system equipment and provides the approach and the associated characteristics to be integrated in an optimization problem that aims to minimize the GMD impacts on power system operation and stability.

A. Impacts of GMDs on Power Transformers

The injection of GIC into the system transformers with grounded neutral saturates the transformer and 1) increases its reactive power demand, 2) turns the transformer into a harmonic current source, and 3) causes hot-spot overheating in the transformer. These effects are further explained below.

1) Increased Reactive Power Loss: When GIC is injected into the transformer, the core magnetizing current and therefore the reactive power demand of the transformer increase due to the directional saturation of transformer. The amount of the GIC-related reactive power loss prominently depends on the transformer core construction [7]–[12] including single-phase, three-phase shell, three-limb, and five-limb. In addition, transformer parameters such as air-core inductance and the inductance of the air-gap between the core and the tank can appreciably influence the reactive power loss of the transformer [9]–[12]. Therefore, an accurate GMD study requires such parameters. However, without loss of generality and for demonstration purpose, the reactive power loss of the study system transformers is simplified to a two-section piecewise linear characteristic for three-limb core transformers and a linear characteristic for the other core constructions.

Based on the definition of a forming function $f(GIC)$, Fig. 1 depicts the characteristics of the system transformers. By taking the slope of the single-phase transformer characteristic as reference, i.e., $s = 1$, the slopes of the shell-type and five-limb cores are assumed 0.7 and 0.8, respectively. The reactive power of the three-limb transformer is negligible up to a threshold current $I_{\rm th}$, beyond which it starts to rise with the slope of 0.77 obtained from the GIC measurements of [9]. The threshold current highly depends on the core knee point and system voltage. Based on data presented in [9], we approximate $I_{\rm th}$ by

$$I_{\rm th} = -55V_{\rm pu} + 63. \tag{1}$$

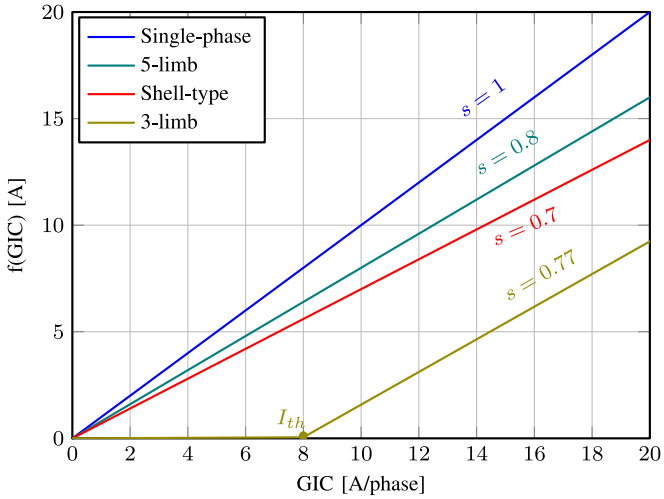

Fig. 1. Forming function to obtain reactive power loss of the system transformers from the applied GIC.

As such, the three phase reactive power loss Q_T of each transformer in MVAR is given by

$$Q_T = 0.001 \times \sqrt{6} V_{\rm Base} V_{\rm pu} f(GIC), \tag{2}$$

which is deduced form the initial characteristic slope rule of single-phase transformers presented in [11]. In (2), $V_{\rm pu}$ is the per-unit voltage of transformer's terminal in the corresponding system base voltage level $V_{\rm Base}$ in kV, and GIC is the magnitude of GIC per phase in amperes. For a network under the duress of a GMD, transformers additional reactive losses due to the flow of GICs should be included as additional reactive loads, at transformer buses, in the power flow analysis. The power flow equations should be solved using the total reactive power. Since the bus voltage and transformer reactive power losses are mutually coupled based on (2), the power flow analysis should be performed in an iteration between power flow equations and (2). As a result of GIC flow and associated excessive reactive losses in transformers, power flow analysis will indicate significant voltage drops and if the GMD is severe enough, the voltage collapse is also likely.

2) Harmonic Current Generation as a Result of GIC: As a result of directional saturation caused by GIC, the transformer current contains both even and odd harmonics with significant magnitudes. Similar to the reactive power loss, the frequency spectrum of the magnetizing current is appreciably affected by the transformer core construction. For the approach of this study, the advanced transformer model of [8], [9], which is the most accurate transformer model for GIC studies [9], [12], has been simulated in time-domain, and the harmonic characteristics of each core construction have been obtained as a function of the applied GIC and the system voltage, for the harmonics up to 25th. Such characteristics are stored in lookup tables and used by the optimization algorithm. The corresponding low order harmonic content of the transformer current versus GIC for various core constructions are shown in Figs. 2, 3, 4, 5. When the power flow solution converges, the harmonics are extracted based on the voltage magnitude obtained from the power flow

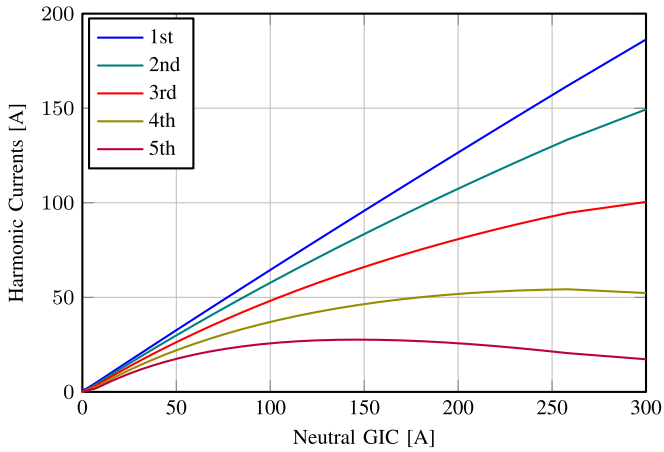

Fig. 2. Low order harmonic content of the transformer current for single-phase transformers versus GIC.

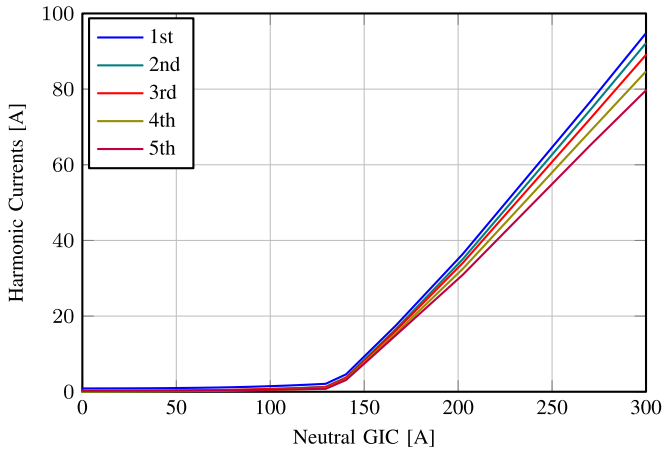

Fig. 3. Low order harmonic content of the transformer current for three-limb three-phase transformers versus GIC.

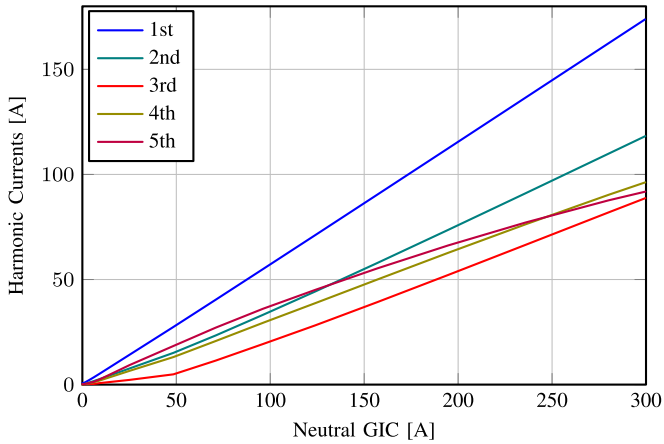

Fig. 4. Low order harmonic content of the transformer current for five-limb three-phase transformers versus GIC.

solution and the GIC obtained from the dc network solution. As discussed later, these harmonics are employed to determine the capacitor bank harmonic overloading and the generator negative sequence current.

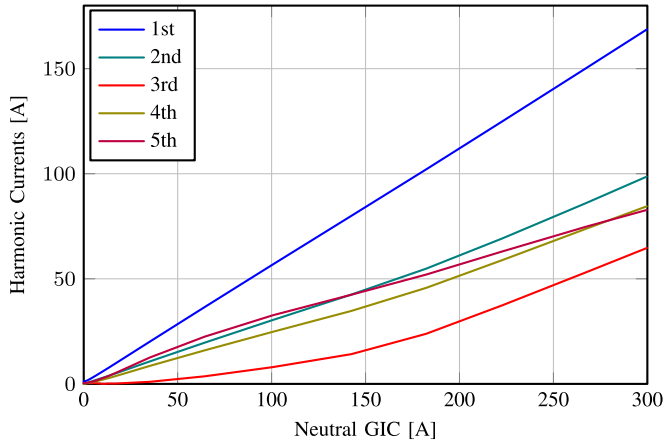

Fig. 5. Low order harmonic content of the transformer current for shell-type three-phase transformers versus GIC.

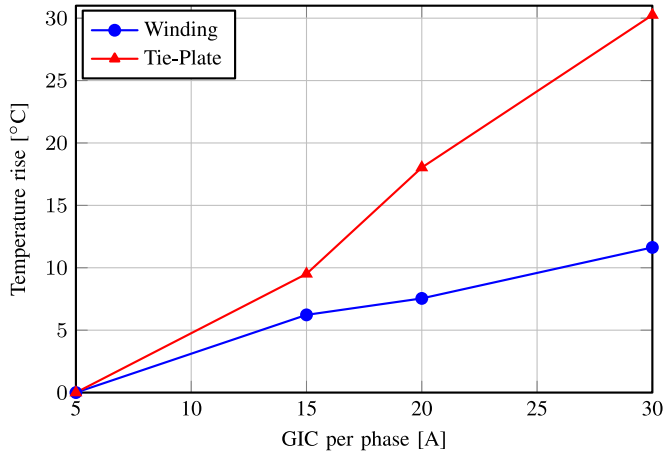

Fig. 6. Steady-state temperature rise of transformer tie-plate and winding at various GIC levels [13]

3) Transformer Hot-Spot Heating: Increase of the out-of-core stray magnetic flux under GIC conditions significantly increases the induced eddy currents in the winding and the core metallic structural parts, such as tie-plate and clamp plates. This results in the hot-spot heating in the windings and the structural parts [13]. When sufficiently high, hot-spot heating can lead to reduced lifespan or even failure of the transformer [1]. However, thermal analysis of the transformer is a challenging and design-dependent problem which should be conducted on case-by-case basis, as the thermal behavior of two transformers with the same core constructions can be significantly different. Furthermore, the hot-spot temperature rise is a time-dependent phenomenon with the associated winding and bulk-oil time constants. Nevertheless, in the power-flow based approach of this study, the transformer spot-heating is taken into account based on the steady-state temperature rise characteristics shown in Fig. 6 [13] noting that higher temperature rises have also been reported in the literature [13]. Assuming the full-load temperature rises prior to the GMD event, the total temperature due to GIC is checked in the proposed mitigation approach to be below the maximum standard permissible values [13].

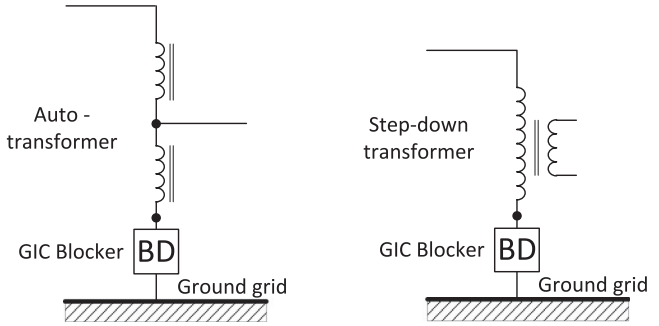

Fig. 7. GIC blockers installed at the neutral points of the autotransformer and step-up/down transformer.

4) Blocking Devices and their Impacts: The impacts of GMDs can be mitigated by installing GIC BDs at the neutral of power transformers, as shown in Fig. 7. Such a device, which is employed in the mitigation approach of this study, represents a high-impedance path for the quasi-dc current and block the flow of GIC in the transformers. In the case of the step-up/down transformer, the GIC is prevented from flowing into the high-voltage (HV) winding of the transformer. However, in an autotransformer, the BD can only block the GIC flow in the common winding while there is still a path from HV terminal to LV terminal through the series winding. Therefore, in the autotransformers, which typically connect two voltage levels of transmission systems, the GIC flows from both HV and LV sides and the neutral GIC blocker for the autotransformers is not as effective as for the step-up/down transformers. In general, an effective GIC should be defined and calculated for the autotransformers as [4]

$$GIC_{\text{eff}} = I_H + \frac{N_{LV}}{N_{HV}}(I_C - I_H), \tag{3}$$

where N_{LV}/N_{HV} is the low-voltage to high-voltage turns ratio and I_H and I_C are the GIC currents of the series and the common windings, respectively.

B. Impacts of GMDs on Transmission Lines

Under no circumstances are the transmission lines allowed to be loaded beyond their short-term emergency ratings and for a pre-specified limited period of time. The conventional Transmission Line Rating (TLR) [14], in both continuous and the post-contingency operating conditions, is determined based on the conductor temperature, which is a function of line current, ambient temperature, and wind speed. However, the conventional ratings are determined at the power frequency. Under the GIC conditions, not only the dc current causes additional power losses and temperature rise in the conductor, but also the harmonic currents generated by the saturated transformers are injected into the transmission lines and generate excess power loss in the conductors. Therefore, to ensure that the transmission line thermal rating is not exceeded, the effects of the dc and the harmonic currents should be accounted for in a thermally equivalent power frequency current $I_{1-\text{eq}}$ when comparing the line duty with the TLR.

If the dc and harmonic currents flowing in the conductor are known, the thermally equivalent current $I_{1-\text{eq}}$ can be defined such that it yields the total power loss which results from all frequency components of the line current:

$$R_1 {I_{1-\text{eq}}}^2 = \sum_{h=0}^{n} R_h(\omega) I_h(\omega)^2, \tag{4}$$

where ω is the angular frequency associated with the hth harmonic, I_h is the hth harmonic current magnitude, R_h denotes the frequency-dependent resistance at the harmonic order h, and R_1 is the conductor resistance at the power frequency, which is typically referred to as R_{ac} in the transmission line conductor specifications [14]. The dc resistance and the dc current are represented by $h = 0$. Therefore, to determine the equivalent power frequency current that produces the same amount of heat as the resultant of all dc, actual power frequency, and harmonic currents, (4) can be rewritten as

$$I_{1-\text{eq}} = \sqrt{\frac{R_{dc}}{R_{ac}} GIC^2 + {I_1}^2 + \frac{R_{dc}}{R_{ac}} \sum_{h=2}^{n} \frac{R_h(\omega)}{R_{dc}} I_h(\omega)^2}, \tag{5}$$

where R_{dc} and R_{ac} and their ratio can be found in the conductor data sheets [14]. The harmonic resistance $R_h(\omega)$ is mainly affected by skin effect with the exact solution based on Bessel functions. However, an approximate expression for $R_h(\omega)/R_{dc}$ ratio is given in [15] as:

$$\frac{R_h(\omega)}{R_{dc}} = \begin{cases} 0.035M^2 + 0.938 & M < 2.4 \\ 0.35M + 0.3 & M \geq 2.4 \end{cases} \tag{6}$$

and

$$M = 0.05012\sqrt{\frac{\mu_r f}{R_{dc}}},$$

where

μ_r: relative permeability of the conductor material
f: frequency in Hz
R_{dc}: DC resistance in Ω/km

C. Impacts of GMDs on Capacitor Banks

Under the GMD conditions, the saturation of the system transformers generates high-magnitude even and odd harmonics. Representing the lower impedance at higher frequencies, the cap-banks can be easily overloaded. The common ungrounded double-wye configuration of capacitor banks blocks the triplen harmonics, i.e., 3rd, 6th, 9th, ..., from entering the cap-bank. However, in a neutral grounded cap-bank, all harmonic components contribute to the capacitor loading.

To calculate the cap-bank harmonic overloading under a GMD, the harmonic currents generated by the transformers should be primarily calculated. Fig. 8 shows the equivalent system representation used for the calculation of the cap-bank harmonics. Any saturated transformer T_j generates the harmonic currents i_{h-Tj} of order h. The cap-bank contribution is deduced as the current division between the cap-bank current i_C and the harmonic currents injected to the system, i_{h-sys}. The harmonic-dependent impedance $Z_{h-\text{Station}}$ seen from the station bus can

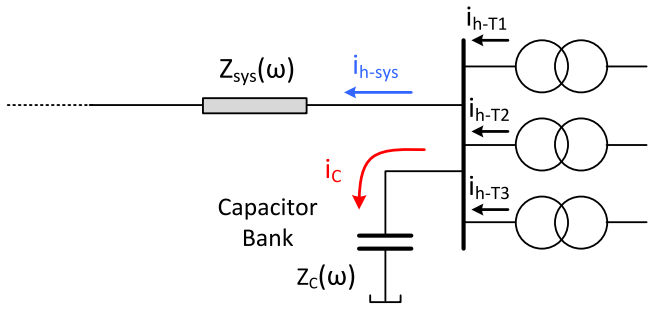

Fig. 8. Equivalent system representation to calculate cap-bank harmonic current contribution.

be deduced as:

$$Z_{\text{Station}}(\omega) = \frac{Z_C(\omega) Z_{sys}(\omega)}{Z_C(\omega) + Z_{sys}(\omega)}, \tag{7}$$

and at each harmonic frequency, the cap-bank harmonic current is given by

$$i_C(\omega) = \frac{Z_{\text{Station}}(\omega) \sum_j i_{h-Tj}(\omega)}{Z_C(\omega)}. \tag{8}$$

The total current i_C then should be calculated and compared with the maximum permissible loading of the cap-bank to ensure it is not exceeded during the GMD.

D. Impacts of GMDs on Synchronous Generators

The increase of the system reactive power demand due to GIC imposes a higher stress on the generator, and if its reactive power capability limit is reached, the generator will not be able to regulate the system voltage. On the other hand, the harmonic and negative sequence currents impose thermal and mechanical stresses on the generator by inducing eddy currents on the rotor surface and causing rotor heating [16]. The rotor heating effect is discussed in [17] which shows that the actual thermal stress during a GMD can exceed the generator capability while the existing standards are unable to address the issue. This is further discussed in this section in more details. In addition to the rotor heating, the negative sequence and harmonic currents also result in the oscillatory torque and vibration of the generator. Therefore, the protection system may alarm or even trip the generator during a GMD, which in turn threatens the power system stability.

The generator operation constraints from power capability standpoint are based on the thermal limits of the different components of the generator. The maximum reactive power delivered by the generator is determined by the field winding thermal capability. The minimum reactive power is deduced based on the minimum excitation level for maintaining the stable operation of the generator and avoiding core end heating. The maximum active power is limited by the armature thermal capability. These generator limits are typically taken into account in power system analyses such as power flow and voltage stability studies.

Generators are typically protected against unbalance and harmonics by negative sequence relays. These relays operate based on an inverse characteristic to ensure the thermal capability curve of the generator, i.e., $I^2t =$ constant. For salient pole and cylindrical synchronous machines, two different IEEE Standards (C50.12 [18] and C50.13 [19]) provide the necessary recommendations. For a salient pole generator, the negative sequence current should not exceed 5% and 10% of the generator rating, with and without amortisseur winding, respectively [18]. For a turbo cylindrical generator [19], the permissible continuous negative sequence for the units up to 350 MVA is 8% and for the larger generators with the rated powers between 351 MVA and 1250 MVA is given by

$$I_2 = 8 - \frac{\text{MVA} - 350}{300} \tag{9}$$

where I_2 is obtained as a percentage of generator rated current and MVA is its nominal output power.

The impact of stator harmonic current on rotor heating is also considered in IEEE standards C50.12 and C50.13. It is recommended to calculate an equivalent negative sequence current that takes into account the combined effects of the negative sequence current and harmonic components in terms of thermal dissipation. In this case, the calculated equivalent current shall not exceed the prescribed values, unless specified by the manufacturer. This equivalent current is given by [18], [19]

$$I_{2\text{eq}} = \sqrt{I_2^2 + \sum_n \sqrt{\frac{n+i}{2}} I_n^2} \tag{10}$$

where $i = +1$ for $n = 5, 11, 17, \ldots$, and $i = -1$ for $n = 7, 13, 19, \ldots$.

The above harmonic components are presented based on three assumptions: i) the system harmonic currents imposed on the generator only include the odd harmonics, ii) the three-phase harmonic currents are balanced, and iii) the effects of triplen harmonics can be ignored because these harmonics are in zero sequence mode and eliminated by the delta winding of the generator step-up (GSU) transformer. However, none of these assumptions are valid under the GMD conditions. The directional transformer saturation due to GIC results in the flow of both even and odd harmonic currents in power system and generators. Furthermore, the three-phase harmonic currents are not balanced in general, particularly when the GSU transformer does not comprise of the single-phase units. As a result, the triplen harmonics can also exist in the generator current. Consequently, the standard equation (10) and its harmonic components are required to be modified for the GMD analysis.

Two options can be pursued to deduce a more realistic equivalent negative sequence current. The first option is to follow the standard Eq. (10) except with the modified harmonic components to include all even and odd harmonics. The associated negative sequence current, hereafter referred to as the modified current $I_{2\text{eq}-\text{mod}}$, is obtained based on the harmonic components

$$n = 3k \mp 1, k = 1, 2, \ldots \qquad \text{with} \quad i = \pm 1 \tag{11}$$

The other option is to take into account the effects of the sequence components of all harmonic currents in the rotor heating assessment. As such, the three-phase harmonic currents I_{hABC}

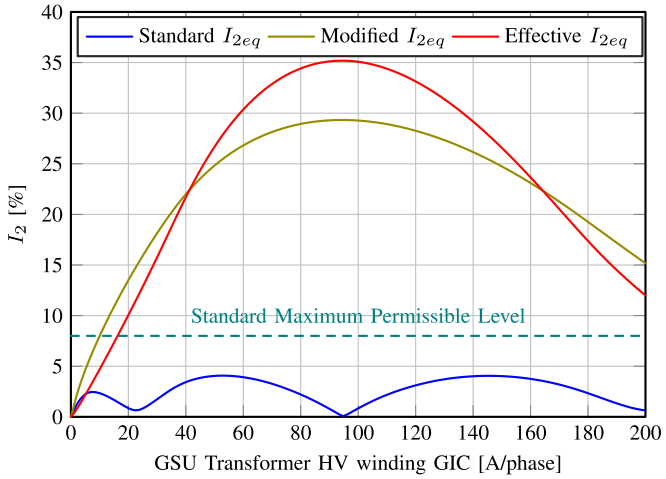

Fig. 9. Comparison between the standard, modified, and effective negative sequence currents of a 100 MVA generator under GIC conditions, with a 345/15 kV GSU transformer having $L_{air-core} = 0.8$ pu (Fig. 10)

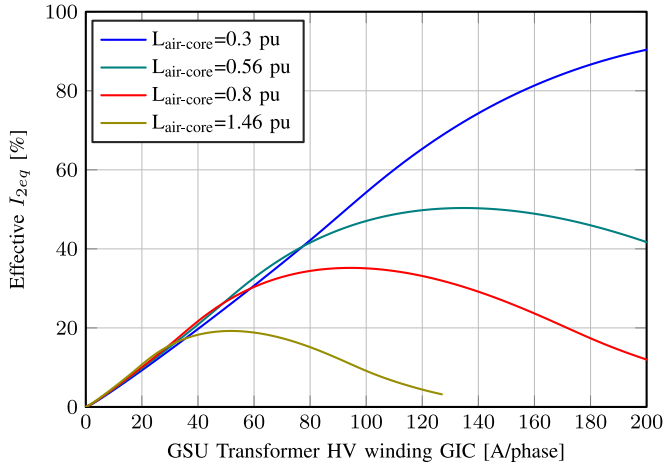

Fig. 10. Impacts of air-core inductance of the GSU transformer on the effective negative sequence current of a 100 MVA generator under the GIC conditions - GSU transformer ratings are assumed 100 MVA − 345/15 kV.

of order h should be converted to sequence domain components according to

$$\begin{bmatrix} I_{h0} \\ I_{h+} \\ I_{h-} \end{bmatrix} = \frac{1}{3} \begin{bmatrix} 1 & 1 & 1 \\ 1 & a & a^2 \\ 1 & a^2 & a \end{bmatrix} \begin{bmatrix} I_{hA} \\ I_{hB} \\ I_{hC} \end{bmatrix} \tag{12}$$

where $a = 1\angle 120^\circ$, and I_{h0}, I_{h+}, and I_{h-} are the zero-, positive-, and negative-sequence components of the current harmonic h, respectively. The zero-sequence currents are negligible and can be ignored due to high-impedance at the generator neutral and the delta connection of the GSU transformer winding. The positive sequence currents generate air-gap fluxes which rotate in the same direction of the rotor revolution with the harmonic frequency h and induce one order lower harmonics on the rotor. In contrast, the negative sequence currents generate the rotating fluxes in the opposite direction and induce one order higher harmonics. As a result, the induced harmonic current of order h on the rotor results from the negative sequence component of one order lower harmonic $I_{(h-1)-}$ and the positive sequence component of one order higher harmonic $I_{(h+1)+}$ of the stator current. Therefore, an accurate effective negative sequence current can be obtained based on the vector summation of the corresponding harmonic phasors as

$$I_{2\text{eq}-\text{eff}} = \sqrt{\frac{{I_{2+}}^2}{\sqrt{2}} + \sum_{h=2} \sqrt{\frac{h}{2}} \left| \overline{I}_{(h-1)-} + \overline{I}_{(h+1)+} \right|^2} \tag{13}$$

where overlines indicate phasor quantities, and noting that I_2 denotes the second harmonic and should not be misinterpreted as the standard fundamental frequency negative sequence current of (9) and (10).

To demonstrate the significance of the proposed negative sequence currents and provide a basis for taking into account the generator heating in a GIC mitigation approach, Fig. 9 compares the equivalent negative sequence currents obtained from the original standard Eq. (10), $I_{2\text{eq}}$, the modified current $I_{2\text{eq}-\text{mod}}$, (11), and the effective current $I_{2\text{eq}-\text{eff}}$, (13) for a 100 MVA generator connected to a 100 MVA–345/15 kV GSU transformer with single-phase core construction and the air-core inductance of 0.8 pu. It is assumed that all the fundamental and harmonic current demand of the GSU transformer under the GIC condition is supplied by the generator.

The simulation results show that when the GSU transformer is subjected to GIC, the standard $I_{2\text{eq}}$ does not exceed 4.1%, even under high GIC magnitudes. This is well below the standard permissible level of 8% which is the basis for the negative sequence relay trip. Thus, under such a condition, the GIC can cause alarming, at most. However, both the modified current $I_{2\text{eq}-\text{mod}}$ and the effective current $I_{2\text{eq}-\text{eff}}$ represent high equivalent negative sequence current and therefore high thermal stress on the rotor, as shown in Fig. 9. $I_{2\text{eq}-\text{mod}}$ and $I_{2\text{eq}-\text{eff}}$ exceed the maximum permissible level at the GIC of 10 A/phase and 16.2 A/phase on the HV side of the GSU transformer, respectively, and can cause the generator trip at these GIC levels. Consequently, the standard $I_{2\text{eq}}$ significantly underestimates the rotor heating and as a result the generator damage is likely.

It should be noted that the unbalanced and harmonic currents and therefore the equivalent negative sequence current of the generator is noticeably influenced by the GSU transformer core construction and parameters [8], [9], [12]. For instance, Fig. 10 depicts the impacts of the GSU transformer air core inductance on the effective negative sequence current. The transformers with relatively lower air-core inductance generate higher magnitude harmonics and consequently higher effective negative sequence currents. However, for simplicity an air core inductance of 0.8 pu is assumed for all GSU transformers in the system under study.

III. Optimal BD Placement in the Study System

As an application, the developed equipment limit characteristics are employed in an optimal BD placement algorithm to mitigate the detrimental effects of GIC. The study system is the IEEE 118-bus benchmark system [6] with complementary data for GMD studies [4].

The BD placement problem should be formulated as an optimization problem to minimize the number of installations and costs and while ensuring no equipment limits and operational constraints are violated. These constraints include power system permissible voltages, generator maximum real/reactive output power, generator rotor heating, transformer hot-spot heating, transmission lines ampacity, and capacitor bank harmonic loading constraints which are formulated within the following BD placement optimization problem:

$$\begin{aligned}
\underset{\mathbf{x}}{\text{minimize}} \quad & C(\mathbf{x}) = \sum_{i=1}^{n} \omega_{\text{VL},i} x_i \\
\text{subject to} \quad & V_i \geq V_{\min}, && i = 1, 2, \ldots, m, \\
& P_{\min_i} \leq P_i \leq P_{\max_i}, && i = 1, 2, \ldots, g, \\
& Q_{\min_i} \leq Q_i \leq Q_{\max_i}, && i = 1, 2, \ldots, g, \\
& I_{2\text{eq}-\text{eff},i} \leq I_{2,i}^{\text{permissible}} && i = 1, 2, \ldots, g, \\
& T_{\text{hot}-\text{spot},i} \leq T_{\text{hot}-\text{spot}}^{\max} && i = 1, 2, \ldots, t, \\
& I_{C,i} \leq I_{C,i}^{\max} && i = 1, 2, \ldots, c, \\
& I_{\text{1-eq,i}} \leq TLR_i && i = 1, 2, \ldots, l,
\end{aligned} \tag{14}$$

where $C(\mathbf{x})$ is the cost function, n is the total number of candidate transformers for BD installation, $\mathbf{x}$ is an n-dimensional binary vector representing the solution of the problem, x_i is the ith element of $\mathbf{x}$ indicating whether BD is installed on the ith transformer, $w_{\text{VL},i}$ is the weighting factor and a function of transformer voltage level, V_i is the voltage of the ith bus, $V_{\min}$ is the minimum permissible voltage level, m is the number of system buses, P_i/Q_i is the real/reactive power generated by the ith generator, $P_{\min_i}$/$P_{\max_i}$ is the minimum/maximum amount of real power that the ith generator can produce, $Q_{\min_i}$/$Q_{\max_i}$ is the minimum/maximum amount of reactive power that the ith generator can produce, $I_{2,i}^{\text{permissible}}$ is the maximum permissible equivalent negative sequence current of the ith generator, g is the number of system generators, $T_{\text{hot}-\text{spot},i}$ is the hot-spot temperature of the ith transformer and $T_{\text{hot}-\text{spot}}^{\max}$ is the maximum permissible temperature [13], t is the total number of transformers in the system, $I_{C,i}$ is the current flowing into the ith capacitor bank and $I_{C,i}^{\max}$ is the maximum permissible, c is the total number of capacitor banks, and l is the number of transmission lines.

In this study, the power limit constraints are taken into account in the power flow analysis subroutine. The other constraints are guaranteed by adding a large penalty term to the cost function in case a constraint is violated. Hence, the constrained optimization problem of (14) is transformed into the following unconstrained optimization problem:

$$\Phi(\mathbf{x}) = C(\mathbf{x}) + P \tag{15}$$

where $P = 0$ if no constraint is violated and $P = 1000$, otherwise. The optimization process is illustrated as a flow chart in Fig. 11.

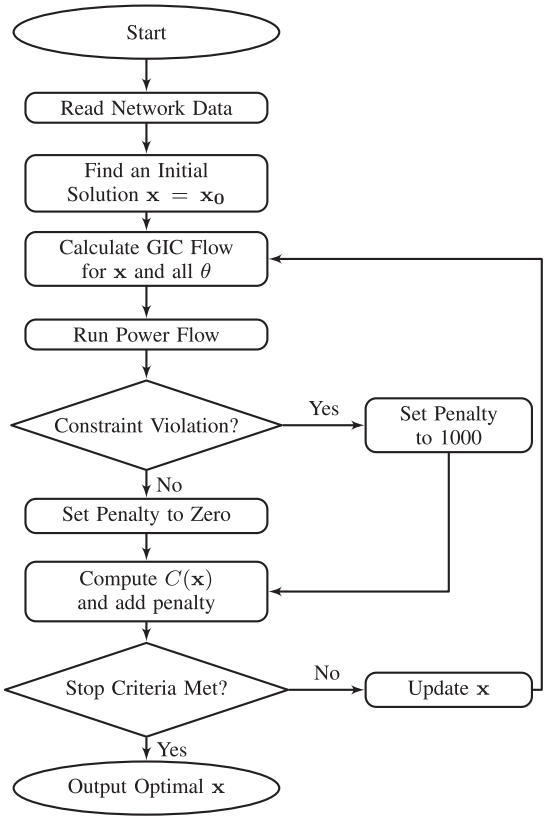

Fig. 11. A flow chart of the optimal BD placement process.

IV. Numerical Results

A. System Impedance Characteristics

Prior to iterative network solution and in order to calculate the capacitor bank harmonic loading, the system-capacitor impedance versus frequency, i.e., $Z_{\text{Station}}(\omega)$ (7), seen from the buses with capacitor banks are required to be obtained. Fig. 12 illustrates such impedances versus harmonics for the total twelve cap-banks of the system under study. Up to 12th harmonic frequency range, some buses show multiple peak impedance values which are associated with resonance conditions at the corresponding frequencies. If a bus impedance peak falls in vicinity of or aligns with a harmonic order, high magnitude of that harmonic is injected into the cap-bank connected to the station bus and therefore the cap-bank is prone to overloading and damage. Under these conditions, the protection system trips the cap-bank. During the optimization process to locate BDs in the study system, it was observed that the cap-banks C_2, C_3, and C_6 are overloaded at relatively lower GMD intensities, due to matching harmonics with the corresponding high impedances. This necessitates the placement of BDs at these capacitors stations. As the GMD intensity increases, more BDs are required to prevent trip of the other capacitors.

B. Optimization Problem Results

The results of optimal BD placement problem are presented in this section. It is assumed that for 345 kV/138 kV transformers $w_{VL,1} = 1.0$/$w_{VL,2} = 0.9$, respectively. Since this is a large-scale, combinatorial, nonlinear, binary integer programming problem, an enumeration approach (or exhaustive search) requires an exorbitant computation time to evaluate all 2^{162} possible combinations. We use the genetic algorithm [20] of MATLAB's optimization toolbox to obtain the optimal

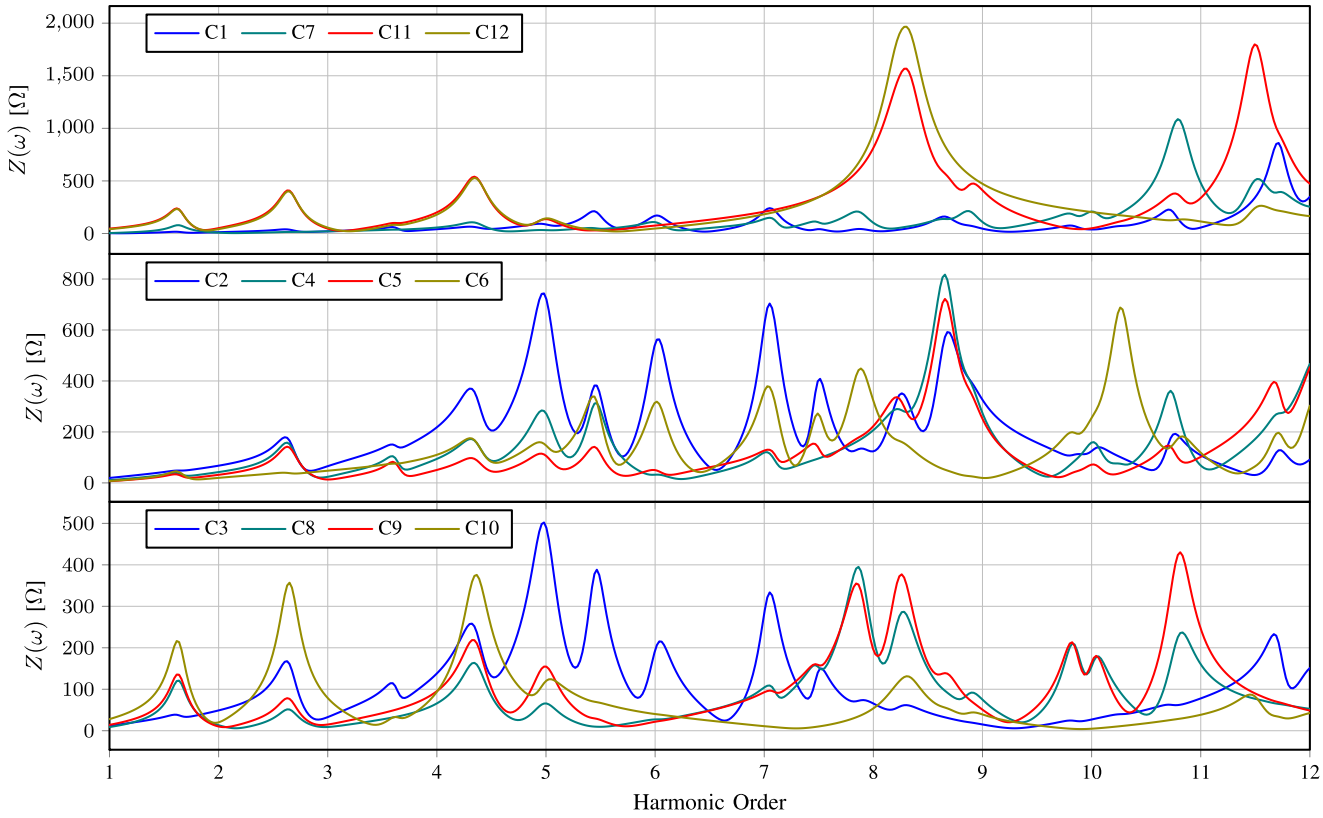

Fig. 12. System impedance various harmonic frequencies seen from the stations with capacitor banks (total twelve capacitor banks in the study system).

TABLE I
OPTIMIZATION RESULTS FOR $E = 1, 2, \ldots, 8$ V/KM

Considered	E V/km							
Equip. Lim.	1	2	3	4	5	6	7	8
None	0	0	5	8	9	11	13	14
Only Cap.	0	31	32	42	45	49	56	69
All	3	97	155	157	158	158	159	159

solution. Due to the stochastic nature of the genetic algorithm, the optimization process is repeated several times, using different parameters and initial solutions, and the best obtained results are presented. The problem is solved for the geoelectric field intensities of 1 V/km to 8 V/km in all possible field directions, i.e., the geoelectric field angle varies from 0 to 360 degrees. It is assumed that the minimum acceptable voltage threshold is $V_{\min} = 0.94$ pu. Since the genetic-algorithm-based optimization process requires numerous computations of the objective function and is computationally burdensome, the problem is solved on a high-performance computer (HPC) featuring 12 processor cores in parallel. Each optimization process would take approximately 25 hours.

The optimization results are presented in Table I. To demonstrate the impacts of considering the equipment thermal limits on the obtained solutions, the results are provided for three cases: i) no equipment limits are considered, ii) only cap-bank limits are considered, and iii) all equipment limits are taken into account. In all these cases, the power-flow (operation limits) including voltage and power constraints are taken into account. As shown in Table I, the results of these cases are significantly different. Unlike the no-thermal-limit case which presents the BD installation as a reasonable solution, the detailed investigation based on the equipment thermal limits presents it as an unacceptable solution. With total 162 transformers in the study system, the results for 3 V/km and beyond show that the BDs should be installed on almost all system transformers.

V. CONCLUSION

The paper presents the equipment thermal limits and the power system operation constraints which should be taken into account in the GMD analysis and proposes a general approach to incorporate these limits in any short-term or long-term GIC mitigating solution. The methods for obtaining the thermal stress on the equipment under various GIC magnitudes are also presented. The proposed GIC mitigation approach determines the BD placement while satisfying the power system operation constraints such as the bus voltage profile and the generator active-reactive power limits. It also takes into account the transformer hot-spot heating, capacitor bank overloading, transmission line loading, and the generator rotor heating limits and provides acceptable solutions.

In addition to the transformers which are the origin of the GMD consequences in power system and subjected to high stress, the simulation results of this study reveal that the

generators can also be at high risk, during GMDs. The simulation results show that while the effective negative sequence current of the generator is well above the maximum permissible level, the corresponding standard equation significantly underestimates the thermal stress. Therefore, the associated protective relay cannot trip the generator under the excessive rotor heating conditions and the generator failure is likely. This paper proposes more accurate equations to determine the rotor heating stress. Compared with a non-constrained problem, the study results show that accounting for the equipment thermal limits leads to noticeably different solutions in the GMD analysis.

REFERENCES

[1] "Effects of geomagnetic disturbances on the bulk power systems," North American Electric Reliability Corporation (NERC), 2012 Special Reliability Assessment Interim Report, 2010_LTRA_V2, Feb. 2012.

[2] "Geomagnetic disturbances: Their impact on the power grid," *IEEE Power Energy Mag.*, vol. 11, no. 4, pp. 71–78, Jul./Aug. 2013.

[3] L. Bolduc, M. Granger, G. Pare, J. Saintonge, and L. Brophy, "Development of a DC current-blocking device for transformer neutrals," *IEEE Trans. Power Del.*, vol. 20, no. 1, pp. 163–168, Jan. 2005.

[4] A. Etemadi and A. Rezaei-Zare, "Optimal placement of GIC blocking devices for geomagnetic disturbance mitigation," *IEEE Trans. Power Syst.*, vol. 29, no. 6, pp. 2753–2762, Nov. 2014.

[5] H. Zhu and T. Overbye, "Blocking device placement for mitigating the effects of geomagnetically induced currents," *IEEE Trans. Power Syst.*, vol. 30, no. 4, pp. 2081–2089, Jul. 2015.

[6] R. Christie, *Power Systems Test Case Archive*, University of Washington, Seattle, WA, USA, Jul. 2013. [Online]. Available: http://www.ee.washington.edu/research/pstca

[7] X. Dong, Y. Liu, and J. Kappenman, "Comparative analysis of exciting current harmonics and reactive power consumption from GIC saturated transformers," in *Proc. IEEE Power Eng. Soc. Winter Meeting*, vol. 1, 2001, pp. 318–322.

[8] A. Rezaei-Zare, "Enhanced transformer model for low- and mid-frequency transients—Part I: Model development," *IEEE Trans. Power Del.*, vol. 30, no. 1, pp. 307–315, Feb. 2015.

[9] A. Rezaei-Zare, "Enhanced transformer model for low- and mid-frequency transients—Part II: Validation and simulation results," *IEEE Trans. Power Del.*, vol. 30, no. 1, pp. 316–325, Feb. 2015.

[10] A. Rezaei-Zare, "Behavior of single-phase transformers under geomagnetically induced current conditions," *IEEE Trans. Power Del.*, vol. 29, no. 2, pp. 916–925, Apr. 2014.

[11] A. Rezaei-Zare, "Reactive power loss versus GIC characteristic of single-phase transformers," *IEEE Trans. Power Del.*, vol. 30, no. 3, pp. 1639–1640, Jun. 2015.

[12] A. Rezaei-Zare, L. Marti, A. Narang, and A. Yan, "Analysis of three-phase transformer response due to GIC using an advanced duality-based model," *IEEE Trans. Power Del.*, vol. 31, no. 5, pp. 2342–2350, Oct. 2016.

[13] L. Marti, A. Rezaei-Zare, and A. Narang, "Simulation of transformer hotspot heating due to geomagnetically induced currents," *IEEE Trans. Power Del.*, vol. 28, no. 1, pp. 320–327, Jan. 2013.

[14] *EPRI AC Transmission Line Reference Book—200 kV and Above*, 3rd ed. Palo Alto, CA, USA: EPRI, 2005.

[15] I. T. F. on Harmonics Modeling and Simulation, "Modeling and simulation of the propagation of harmonics in electric power networks," *IEEE Trans. Power Del.*, vol. 11, no. 1, pp. 452–474, Jan. 1996.

[16] W. Gish, W. Feero, and G. Rockefeller, "Rotor heating effects from geomagnetic induced currents," *IEEE Trans. Power Del.*, vol. 9, no. 2, pp. 712–719, Apr. 1994.

[17] A. Rezaei-Zare and L. Marti, "Generator thermal stress during a geomagnetic disturbance," in *Proc. IEEE Power Energy Soc. Gen. Meeting*, Jul. 2013, pp. 1–5.

[18] IEEE *Standard for Salient-Pole 50 Hz and 60 Hz Synchronous Generators and Generator/Motors for Hydraulic Turbine Applications Rated 5 MVA and Above*, IEEE Standard C50.12-2005 (Previously designated as ANSI C50.12-1982), pp. 1–45, Feb. 2006.

[19] *IEEEStandard for Cylindrical-Rotor 50 Hz and 60 Hz Synchronous Generators Rated 10 MVA and Above*, IEEE Standard C50.13-2014 (Revision of IEEE Std C50.13-2005), pp. 1–63, May 2014.

[20] M. Mitchell, *An Introduction to Genetic Algorithms*. Cambridge, MA, USA: MIT Press, 1996.

Afshin Rezaei-Zare (M'08–SM'10) received the B.Sc., M.Sc., and Ph.D. degrees (Hons.) in electrical engineering from the University of Tehran, Tehran, Iran, in 1998, 2000, and 2007, respectively. He was a Visiting Scientist from 2005 to 2007, and a Postdoctoral Fellow from 2007 to 2009 at the Department of Electrical and Computer Engineering, University of Toronto, Toronto, ON, Canada. From 2010 to 2017, he was with the Department of Special Studies, Hydro One Networks Inc., Toronto. In 2017, he joined the Department of Electrical Engineering and Computer Science, York University, Toronto. His research interests include the development of new models for the electromagnetic transient programs, analysis of electromagnetic transients in transmission and distribution power systems and apparatus, numerical solution techniques, power grid resilience, and renewable and smart energy systems. Prof. Rezaei-Zare is a registered Professional Engineer in the Province of Ontario, Canada, and an Editor of the IEEE TRANSACTIONS ON POWER DELIVERY.

Amir H. Etemadi (S'08–M'12) received the B.Sc., M.Sc., and Ph.D. degrees in electrical engineering from The University of Tehran, Sharif University of Technology, Tehran, Iran, and the Ph.D. degree from the University of Toronto, Toronto, ON, Canada, in 2005, 2007, and 2012, respectively. He is currently an Assistant Professor with the Department of Electrical and Computer Engineering, The George Washington University, Washington, DC, USA. His research interests include distributed generations and power system dynamics and control.